Methods 66 (2014) 237–245

Contents lists available at ScienceDirect

Methods

journal homepage: www.elsevier.com/locate/ymeth

Revealing molecular structure and orientation with Stokes vector resolved second harmonic generation microscopy

Nirmal Mazumder [a], Chih-Wei Hu [a], Jianjun Qiu [a], Matthew R. Foreman [b,c], Carlos Macías Romero [d], Peter Török [b], Fu-Jen Kao [a,*]

[a] Institute of Biophotonics, National Yang-Ming University, Taipei 11221, Taiwan, ROC
[b] Blackett Laboratory, Department of Physics, Imperial College London, Prince Consort Road, London SW7 2BZ, UK
[c] Max Planck Institute for the Science of Light, Günther-Scharowsky-Straße 1, 91058 Erlangen, Germany
[d] Ecole Polytechnique Fedérale de Lausanne (EPFL), Lausanne, Switzerland

ARTICLE INFO

Article history:
Available online 25 July 2013

Keywords:
Optical scanning microscopy
Second harmonic generation
Stokes vector
Ultrafast laser

ABSTRACT

We report on measurements and characterization of polarization properties of Second Harmonic (SH) signals using a four-channel photon counting based Stokes polarimeter. In this way, the critical polarization parameters can be obtained concurrently without the need of repeated image acquisition. The critical polarization parameters, including the degree of polarization (DOP), the degree of linear polarization (DOLP), and the degree of circular polarization (DOCP), are extracted from the reconstructed Stokes vector based SH images in a pixel-by-pixel manner. The measurements are further extended by varying the polarization states of the incident light and recording the resulting Stokes parameters of the SH signal. In turn this allows the molecular structure and orientation of the samples to be determined. Use of Stokes polarimetry is critical in determination of the full polarization state of light, and enables discrimination of material properties not possible with conventional crossed-polarized detection schemes. The combination of SHG microscopy and Stokes polarimeter hence makes a powerful tool to investigate the structural order of targeted specimens.

1. Introduction

Second harmonic generation (SHG), a second order nonlinear coherent optical process, has been widely used for imaging non-centrosymmetric molecular structures, partly due to the lack of photobleaching [1–8]. SHG provides a unique contrast mechanism on a wide range of materials, as well as the capacity to image with higher spatial resolution and at sub-millimeter depths [1–5]. SHG imaging is commonly used in conjunction with two-photon-excited (TPE) fluorescence for optical diagnostics on complex cellular assemblies, such as skin or organ tissues [6,7]. Recently, polarization resolved SHG microscopy was used to investigate the relative molecular orientation and disorder in the structure of human tissues, such as the dermis [9], cornea [10,11], and myosin of the skeletal muscle [12–14]. SHG anisotropy was studied through the measurement of the SH intensity whilst rotating the polarization of the incident linearly polarized excitation beam [2,4,15,16]. The nonlinearity of SH enables a higher extinction ratio in polarization microscopy, as can prove beneficial in, for example, overcoming the depolarization due to high NA optics [17]. In general, multiphoton microscopy is expected to enhance polarization effects induced on the sample, especially for nonlinear optical contrasts based upon higher order susceptibilities.

Polarization analysis of a SH signal can be carried out using either Jones calculus or Stokes algebra [18]. In most applications cross-polarized two-channel detection is employed and hence use of Jones calculus is used. Strictly, the Jones method is however, only applicable for perfectly polarized light beams [18,19] and is thus unsuitable in many scenarios. For example, use of cross-polarized two-channel detection does not allow the relative ratio of the polarized and un-polarized components of the field to be determined. Additionally, the full polarization state of the polarized component cannot be found due to an ambiguity over the phase difference between the two measured polarization basis vectors. In contrast, the full polarization state of a general optical signal, including partially polarized or unpolarized fields, can be characterized using Stokes algebra [20,21]. Accordingly, a four-channel Stokes polarimeter can be constructed so as to measure all four Stokes parameters. In this article, Stokes vector based SHG microscopy is therefore reviewed [22–24]. Knowledge of the optical polarization properties of biological tissues, which can be inferred from a set of measured Stokes parameters, has a number of biomedical applications since it provides insight into molecular

* Corresponding author. Fax: +886 2 28235460.
E-mail address: fjkao@ym.edu.tw (F.-J. Kao).

1046-2023/$ - see front matter © 2013 Elsevier Inc. All rights reserved.
http://dx.doi.org/10.1016/j.ymeth.2013.07.019

structure and tissue organization. The polarization parameters can for instance, be correlated with the corresponding structural symmetry of tissue samples. A full Mueller matrix formalism, a 4×4 matrix, has long been shown as a powerful method in the context of linear optics [24]. However, in the case of nonlinear optics, the Mueller matrix formalism and associated physical interpretation [24], including the decomposition and the corresponding interpretation, are very involved and may be counter-intuitive [25]. Therefore, developing a full formalism of nonlinear optics based Mueller matrix for correlating the polarization states of the input beam with the nonlinear output optical signals, despite of the envisioned beauty of such a theory, is likely beyond practicality. Although we believe the presented treatment to be generally applicable, we choose to demonstrate it through characterization of the polarization properties of SH signal from potassium m dihydrogen phosphate (KDP) and type-I collagen.

2. Materials and methods

2.1. Instrumentation

A schematic diagram of an experiment arrangement, suitable for measuring the polarization properties of SH signal of SHG microscopy, is described in detail in [22,23] and is shown in Fig. 1. The illumination and excitation optics, used to generate a SH signal from a sample of interest, is very much the same as other multiphoton microscope, and is formed by integrating an ultrafast laser with a scanning microscope. The detection optics, comprising a Stokes polarimeter incorporated into the output of a scanning microscope (operating in a transmitting modality), and the associated calibration is, however, the main focus of this work.

A femtosecond Ti: Sapphire (Coherent Mira Optima 900-F) laser oscillator was used to generate linearly polarized ~150 fs pulses with central wavelength of 800 nm and average power ~550 mW at a repetition rate of ~76 MHz. Our polarization setup includes a polarization state generator (PSG), sample and polarization state analyzer (PSA). The various linear and circular polarization states are generated using the PSG, which is a combination of a linear polarizer (LPUV 100-MP, Thorlabs), a half wave-plate ($\lambda/2$) (AHWP05M-600, achromatic HWP, Thorlabs), and a quarter wave-pate ($\lambda/4$) (AQWP05M-600, achromatic QWP, Thorlabs). A dichroic mirror reflects the laser pulses into the microscope objective lens (UPlanFLN 40X/N.A. 1.3, Olympus Co., Japan). In our experiment, the diameter of the laser beam before the objective lens is 5 mm, which is less than the back aperture of the objective lens, which is approximately 10 mm. We chose not to fill the aperture such that (1) transmission loses and (2) depolarization associated with high NA focusing was reduced. The laser beam was focused onto a sample mounted upside-down on an XYZ stage and scanned with a laser scanning unit (Olympus, FV300). Collected SH signals were analyzed by our polarization state analyzer (PSA), commonly known as a four-channel Stokes-polarimeter.

2.2. Working principle of four channel Stokes-polarimeter

Of great importance in this work are the Stokes parameters on the light scattered from a sample, regardless of whether their origins are attributed to linear or nonlinear process. As mentioned earlier, there is no well accepted theory or formalism on nonlinear optics based Mueller matrix. We would like to point out that Mueller matrix formalism becomes a practical approach only when Lu-Chipman decomposition [24] is also implemented to make a functional connection between the input and output polarization states. For nonlinear optics, the corresponding decomposition method does not exist and would regardless be overwhelmingly complicated to be intuitive and practical. Fig. 2 shows the schematic in explaining the difference between Stokes polarimetry, as compared to Mueller polarimetry. Given the discussion above, a full Mueller matrix formalism remains a powerful method only within the context of linear optics [24,26].

A Stokes polarimeter consists of a light source (in our case the SH signal), polarization state analyzer (PSA) and intensity based detection (I). Specifically, a Stokes polarimeter measures the polarization state of the incoming optical signal, as parameterized by the associated Stokes parameters, or collectively the Stokes vector $S_{out} = [S_0, S_1, S_2, S_3]^t$. Each Stokes parameter can be accorded a physical meaning by noting [27,28].

$$S = \begin{bmatrix} S_0 \\ S_1 \\ S_2 \\ S_3 \end{bmatrix} = \begin{bmatrix} I_{0^\circ} + I_{90^\circ} \\ I_{0^\circ} - I_{90^\circ} \\ I_{45^\circ} - I_{-45^\circ} \\ I_{RCP} - I_{LCP} \end{bmatrix} \quad (1)$$

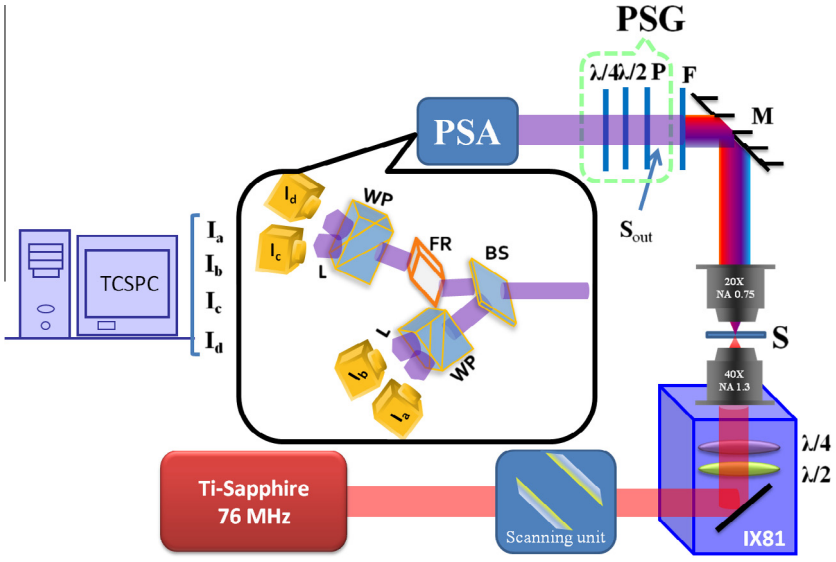

Fig. 1. The schematic diagram of polarization resolved second harmonic generation four-channel Stokes-polarimeter setup. The setup is module based. PSG is inserted for the calibration of PSA and is removed afterward. $\lambda/2$: half wave-plate, $\lambda/4$: quarter wave-plate, S: sample, M: mirror, F: filter, BS: Beam splitter, FR: Fresnel rhomb, WP: Wollaston prism, L: focusing lens, I_a, I_b, I_c, I_d: photo-multiplier tubes (PMTs), TCSPC: Time correlated single photon counting.

Table 1
The fitting parameters of the Stokes vectors scale quadratically with the incident power measured at 4 ROIs (R1–R4).

Region of interest (ROI)	Log <S_0>, F(x)	Log <S_1>, F(x)	Log <S_2>, F(x)	Log <S_3>, F(x)
R1	1.988*x-3.873	2.0676*x-3.896	1.989*x-4.06	2.013*x-4.333
R2	1.963*x-4.306	1.811*x-5.783	1.904*x-5.081	1.917*x-5.196
R3	2.102*x-7.189	2.123*x-4.982	1.738*x-6.403	2.075*x-5.569
R4	2.109*x-4.389	2.111*x-4.183	2.034*x-4.255	2.032*x-4.453

such that S_0 is the total intensity, S_1 is the intensity difference between the linearly polarized states at 0° and 90°, S_2 is the intensity difference between the linearly polarized states at 45° and −45°, and S_3 is the intensity difference between the right-handed (RCP) and left-handed (LCP) circularly polarized states, respectively.

The measured Stokes vector can be expressed as $S_{out} = (A_{4\times4})^{-1} \cdot I$ where $A_{4\times4}$ is known as the instrument matrix of the polarimeter, S_{out} is the Stokes vector of the SH light, and $I = [I_a, I_b, I_c, I_d]^t$, is a vector of the detected intensities measured in each arm of the polarimeter. For comparison, a Mueller polarimeter consists of a PSG, sample (with an associated Mueller matrix M) and PSA. The Mueller matrix, M, describes how the linear interaction of light with the sample changes the polarization state of input Stokes vectors "S_{in}" to the output Stokes vector "S_{out}" by, $S_{out} = M \cdot Sin$. Full determination of the Mueller matrix requires sequential input of different polarization, such that S_{out} and S_{in} become matrix quantities. Accordingly the Mueller matrix, M, of the sample can then be found using, $M = Sout...I.(S_{in})^{-1}$ The Stokes-Mueller matrix formalism is widely used in linear optical measurements [29–32], however the equivalent inversion equation does not exist. In the cases of nonlinear microscopy e.g. SHG, CARS, the interactions are nonlinear and cannot be characterized with a simple 4×4 matrix. If a Mueller matrix is used in the case of second order nonlinear optical process, a 9×1 input Stokes vector is needed and the corresponding Mueller matrix becomes 4×9 [25]. Nevertheless, Stokes polarimetery can be performed regardless of whether the optical signal is linear or nonlinear in origin because only the polarization states of the output light matters. The Stokes parameters can, fortunately, still be used to retrieve crucial and valuable information regarding the sample.

Fig. 1 shows the four-channel Stokes-polarimeter imaging configuration. The SH signal (centrally peaked at 400 nm) was collected in the forward direction by a 20X, 0.75 N.A. objective lens (Olympus Co., Japan). A combination of a band pass filter of 400 ± 40 nm (Edmund Optics Inc. Barrington, New Jersey) and a 680 nm short pass filter (Brightline 680 SP, Semrock) were inserted in the SH emission path. The forward collected SH signal was analyzed by a Stokes polarimeter as discussed above. The SH signal passes through different optics and electronics as shown in Fig. 1, a beam splitter (BS), Wollaston prisms (W1 and W2; WP 10, Thorlabs), Fresnel rhomb (FR; FR 600 QM, Thorlabs) and photon counting photo-multiplier tubes (PMTs; PMA 185 model, PicoQuant GmbH, Berlin, Germany). Firstly, the SH signal is divided into two parts by a beam splitter, which are then split further by two Wollaston prisms oriented at 45° with respect to the plane of incidence. One part, before separation by W2, is passed through a Fresnel rhomb, acting as an achromatic quarter wave plate so as to enable analysis of circularly polarized components. The output of the Stokes polarimeter, a total of 4 channels, is then coupled to the photon counting PMTs through high transparency liquid light guides of 5 mm core diameter (LLG0538-6, Thorlabs Inc.).

The four SH intensities (counts per msec) are detected by TCSPC simultaneously, as shown in Fig. 1. The 2D Stokes vector images 'S_{out}' are reconstructed from the four SH signal intensity images acquired with 256 × 256 pixels spatial resolution, which corresponds to a 50× 50 μm scanning area, using a pixel dwell time of 8 μs. The SH signals were processed by four-channel detector router time-correlated single-photon counting electronics (TCSPC, PHR 800, PicoHarp300, PicoQuant GmbH, Berlin, Germany). Data collection and primary analysis were achieved by a commercial software package (SymPhoTime, PicoQuant GmbH, Berlin, Germany). A series of bespoke MATLAB (MathWorks, R2009b) programs were developed to fully reconstruct the data.

In spite of the lack of a nonlinear optics based Mueller matrix formalism, crucial physical parameters of the detected light can be inferred from the measured Stokes parameters [27], including the degree of polarization (DOP), degree of linear polarization (DOLP) and degree of circular polarization (DOCP) as defined respectively as:

$$\begin{aligned} DOP &= (S_1^2 + S_2^2 + S_3^2)^{1/2}/S_0 \\ DOLP &= (S_1^2 + S_2^2)^{1/2}/S_0 \\ DOCP &= |S_3|/S_0 \end{aligned} \quad (2)$$

DOP indicates the intensity fraction of the light which is fully polarized and ranges from 0 to 1. A DOP value of unity corresponds to perfectly polarized light, whereas a zero DOP corresponds to unpolarized light. For unpolarized light the Stokes parameters are $S_0 = 1$, $S_1 = S_2 = S_3 = 0$. For partially polarized light the DOP lies between 0 and 1 [27]. The DOLP similarly describes the fraction of light which is fully linearly polarized; DOLP is 0 if the light is

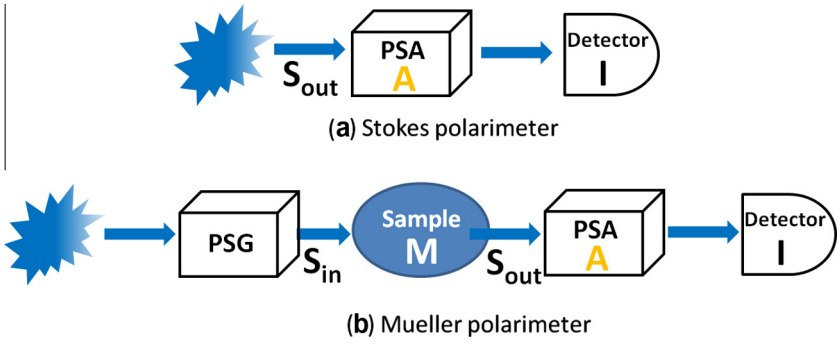

Fig. 2. (a) A Stokes polarimeter measures the polarization state of a light signal using a Polarization State Analyzer (PSA); (b) A Mueller polarimeter characterizes the sample properties and the polarization state of light, specifically by considering how the polarization state (generated by a Polarization State Generator, PSG) is changed by the sample (M).

not linear polarization light and 1 for perfectly linear polarization. The DOCP is a measure of how effectively the birefringence property changes within the sample; DOCP values lies in between 0 and 1.

3. Results and discussion

3.1. Calibration

The four-channel Stokes-polarimeter, optimized for operation at 400 nm, was designed following Azzam et al. and Török et al. [17,28,33], which is a four-detector based setup and is capable of determining all the Stokes parameters of the detected signal simultaneously. The Stokes parameters of the SH signals generated by an unknown sample can, however, only be accurately measured if the instrument matrix '$A_{4\times4}$' of PSA is well known. A calibration protocol in which known polarization states are input into the PSA must hence first be performed so as to determine the instrument matrix. Specifically, for calibration, we generate SH light at 400 nm by focusing the 800 nm laser beam onto KDP micro-crystals (SIGMA, Germany) sandwiched between two cover glass slips and immersed in oil, for optimal index matching. The so-generated SH light is subsequently collimated by a 20 × 0.75 NA objective lens. Linearly and circularly polarized states, 0°, 90°, 45° and LC are then generated using a PSG placed after the collimating lens (for calibration purposes only). The Stokes polarimeter is calibrated using the self-calibration eigen-value method (ECM) [33,34], with the 0°, 90°, 45° and LC input polarization states [22,33,34]. The accuracy of the measurements were determined by the condition number of the instrument matrix '$A_{4\times4}$', which is defined as $C = \|A_{4\times4}\| \cdot \|(A_{4\times4})^{-1}\|$ where $\|\cdots\|$ denotes the L^2-norm. In order to maintain high measurement accuracy, the condition number should be as low as possible [33,35]. A typical computed instrument matrix '$A_{4\times4}$' for our four-channel Stokes polarimeter, as found by the calibration routine describe above, at 400 nm is given by:

$$A_{4\times4} = \begin{bmatrix} 181.0489 & -96.0745 & -165.8139 & 4.6143 \\ 240.9287 & -112.7777 & 192.6028 & 4.8718 \\ 234.4582 & 86.8584 & -19.2318 & -194.0842 \\ 314.7530 & 98.7245 & 28.8309 & 286.7345 \end{bmatrix} \quad (3)$$

Typically a tuned PSA achieves a condition number of the instrument matrix in Eq. (3) of around 2.8 [36]. The errors in the measurement are attributed to electronic and shot noise and may be further reduced through pixel-binning, increasing the acquisition time, or cooling the PMTs. The PSG is removed once the microscope setup, including PSA, is calibrated. The SH signals are processed by TCSPC electronics. The TCSPC module recorded the pixel position of each emitted photon with temporal correlation, which is then used for time-gated image reconstruction [37]. Single photon counting events were recorded using time tagged time resolved (TTTR) protocol [38]. The time gating capacity would allow the rejection of short wavelength autofluorescence from SH. We have also developed a series of MATLAB (MathWorks, R2009b) programs based on the TTTR protocol to reconstruct the photon counting events collected through the four channel setup into Stokes vector based data sets. The resulting spatially resolved SH micrographs permit detailed analysis of the type I phase matching and the general symmetry properties of a SH active sample [23].

Fig. 3 shows the experimental normalized Stokes vector images of the SH light after the PSG, that were in turn detected by the polarimeter. The normalized Stokes vector at each pixel in the scanned area is defined as:

$$\hat{S}(x,y) = S(x,y)/S_0(x,y) = [\,1 \quad \hat{S}_1(x,y) \quad \hat{S}_2(x,y) \quad \hat{S}_3(x,y)\,]^T \quad (4)$$

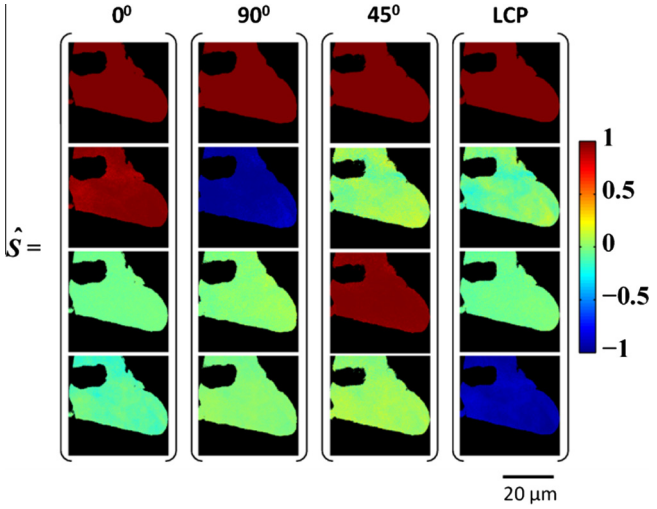

Fig. 3. The normalized 2D reconstructed Stokes images from KDP micro-crystals for input polarization states correspond to 0°, 45°, 90° linear, and LC polarization, respectively. The color scale shows the values of each parameter increasing from -1 (blue) to 1 (red).

It is evident from Fig. 3 that the values of the Stokes parameters of the given polarization state are close to the theoretical values of the normalized Stokes vectors for 0°, 45°, 90°, LCP are $[1,1,0,0]^T$, [1,−1,0,0]T, $[1, 0, 1, 0]^T$, $[1, 0, 0, -1]^T$, respectively. We have also checked the uniformity of the SH signal at the focal plane of the liquid light guide by moving the position of KDP micro-crystals at five different points in the same scanning field of view. We have observed that the values of the Stokes parameters remain the same, irrespective to the position of the crystal [Movie1].

3.2. SHG polarization resolved imaging of KDP micro-crystals and type-I collagen

The capability and performance of the Stokes polarimeter is validated through a series of experiments by obtaining SH signal from KDP micro-crystals (SIGMA, Germany) and type-I collagen (Bovine Achilles Tendon, SIGMA, Germany). We investigated the SH signals by using Stokes parameters based image analysis techniques to determine the SHG contrast in KDP micro-crystals and type-I collagen, as well as to examine the molecular alignment and orientation through angular dependency measurement. The samples were sandwiched between two cover glass slips. The average powers of the laser on the sample surface were ∼0–3 mW and ∼12 mW for KDP micro-crystals and type-I collagen, respectively.

3.2.1. Characterization of Stokes parameter of SH signal w.r.t. incident power

In order to characterize the collected SH light, we performed an experiment to determine the dependence of the signal strength upon the incident power. The effect of the incident power and the polarization angle on the Stokes parameters and the corresponding polarization parameters was also investigated. Fig. 4 shows the 2D reconstructed Stokes vector and the DOP, DOLP, and DOCP images of SHG light collected from a single KDP micro-crystals domain. The Stokes parameters are seen to vary in different areas of the image. In Fig. 4(a), the Stokes parameter (S_0) shows the SHG intensity image. These images were reconstructed using pixel based analysis without relying on any sample alignment. We selected four different region of interests (ROIs) (R1, R2, R3, and R4), each with 10 × 10 pixels, from the Stokes vector images for comparison. The Stokes parameters and the

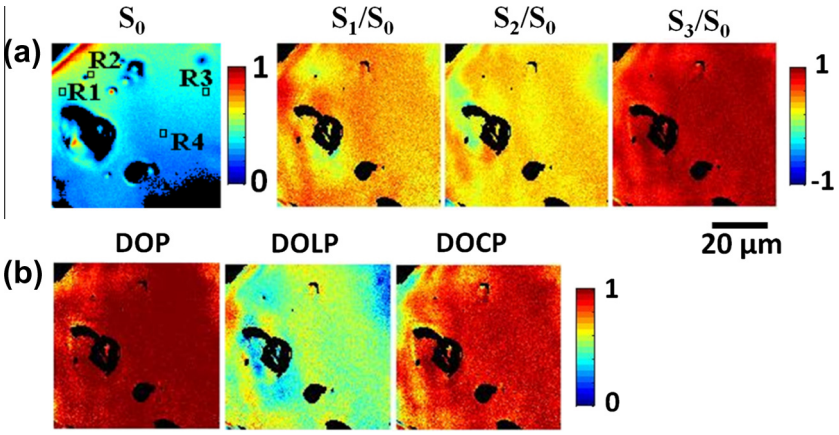

Fig. 4. Experimental polarization resolved 2D images reconstructed from SH response from KDP micro-crystals, (a) shows the reconstructed 2D Stokes vector images; (b) represents the DOP, DOLP, and DOCP images of SHG light from the KDP micro-crystals, when the input polarization is horizontally polarized. The color scale shows the values of each parameter.

corresponding polarization parameters within each ROI were averaged to improve the signal to noise ratio (SNR).

Fig. 5 shows the dependency of the average values of the Stokes parameters ($\langle S_0\rangle$, $\langle S_1\rangle$, $\langle S_2\rangle$ and, $\langle S_4\rangle$) on the incident laser power measured in the 4 ROIs indicated in Fig. 4(a). These graphs show the linear data fitting (See Table 1) of the average Stokes parameters and the incident power on a log scale. In the graphs, the points represent experimental results whilst the solid lines show the mean values corresponding to each polarization parameter. The data fitting results show that SH intensity (S_0) scales quadratically with the illumination power as would be expected for a second order process [39]. Similarly, the Stokes parameters are also proportional to the square of the incident power as shown in Fig. 5. The fluctuations of average values of Stokes parameters are relatively higher if one of the values is smaller than the others due to noise amplification in the processing algorithms [40]. The Stokes parameters values are different in each of the 4 ROIs. This may be due to the relative phase shift between the extraordinary and the ordinary rays and the orientation of the crystals within the depth of field of view of the objective [17,40,41].

Fig. 6 shows the dependence of different physical parameters such as DOP, DOLP and DOCP reconstructed from Stokes parameters in 4 ROIs as shown in Fig. 4. It is expected that the polarization parameters be independent of the incident power for a single domain in KDP crystal but to vary in different ROIs. As shown in the graph, the measured ⟨DOP⟩, ⟨DOLP⟩, and ⟨DOCP⟩ values remain constant irrespective of the incident powers in agreement with expectations. Variation of these parameters between different ROIs is also clearly evident. Generally, the ⟨DOP⟩ values in all the 4 ROIs are ~1, due to the coherent nature of SHG process. Furthermore, the circularly polarized component is seen to constitute a greater proportion of the total power. For example, ⟨DOCP⟩ is seen to be approximately equal to ⟨DOLP⟩ in R1, but much higher in R2, R3, and R4. This can be explained by the phase retardation and the crystal orientation caused by birefringence of the KDP crystals [17].

3.2.2. Polarization resolved SHG imaging in collagen

Type-I collagen is a triple helix, which is approximately 300 nm in length and 1 nm in width. The helix is connected by two polypeptide chains [42]. Collagen fibers produce a strong SH signal,

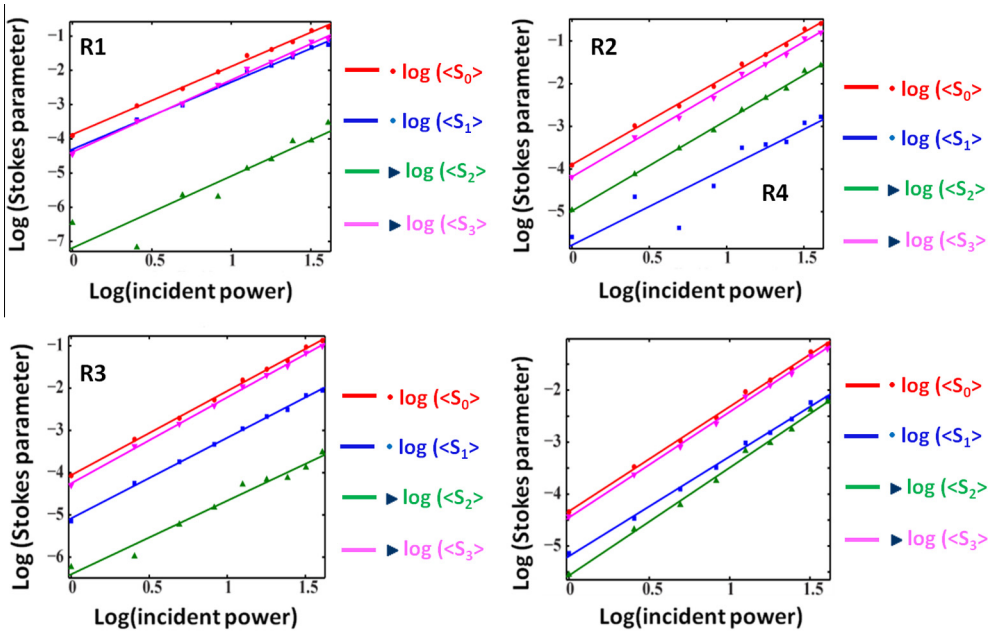

Fig. 5. The Stokes parameters scale quadratically with the incident power measured at 4 ROIs (R1–4), as shown in Fig. 4.

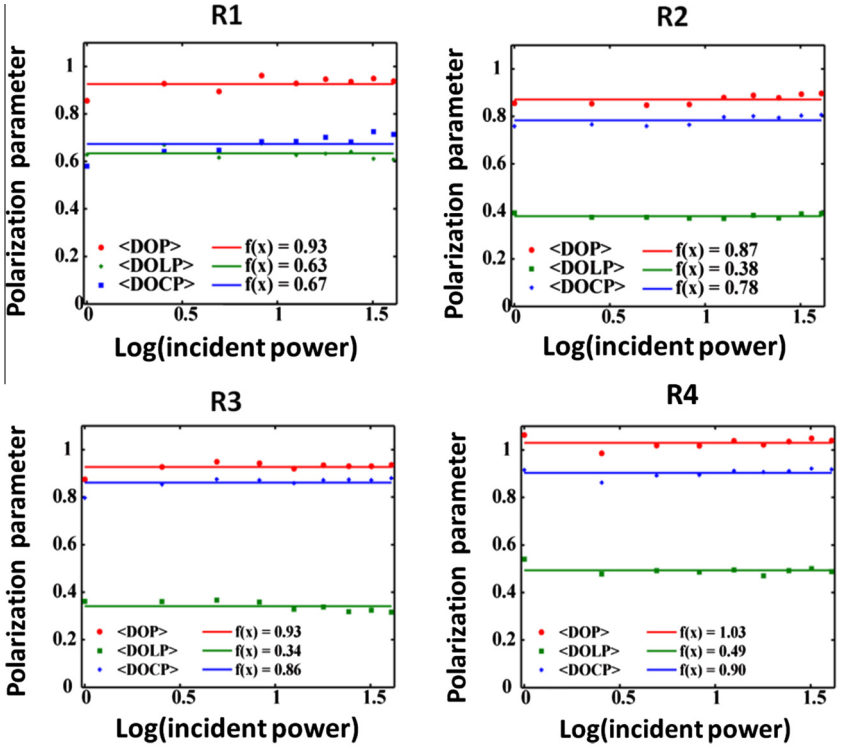

Fig. 6. shows the DOP, DOLP, DOCP of SH light from KDP micro-crystals with the illumination power measured at 4 ROIs (R1–4), as shown in Fig. 4.

which allows easy discrimination of collagen in biological tissue imaging [3,9,43]. The second-order nonlinearity was claimed be enhanced, attributed to the helical and superhelical structures [44]. Consequently, for over a decade, biomedical problems have commonly been studied via of SHG microscopy of type-I collagen [3–5]. We have investigated the SHG signal from type-I collagen by using Stokes parameters based image analysis techniques described above to determine image contrast as well as to examine the molecular alignment in each fiber. Collagen fibers and muscles are naturally occurring birefringent biomaterials in tissues. Conventional polarization microscopes are hence frequently used to detect and study this birefringence [45]. Birefringence arising through χ^2 is, however, greatly enhanced under second harmonic imaging, therefore motivating the use of SHG polarization imaging of collagen fiber for structural assessment, as shown in Fig. 7. Fig. 7(a) shows the normalized Stokes vector images of the SH signal obtained from type-I collagen fibers, with under a horizontally polarized illumination. In particular, the Stokes parameters show that the polarization states of SH light varies between each image pixel. Upon interaction with the collagen fibers, the horizontally polarized excitation beam was transformed into polarization states ranging from linearly to circularly polarization. Similarly to above, Fig. 7(b) shows the spatial variation of the SH light from the DOP, DOLP and DOCP images.

With reference to Fig. 7(b), it is evident that the SH signal generated within the collagen fibers can become partially polarized (as parameterized by the DOP) due to the scattering from inhomogeneities within the sample [41]. We again note, as above, that the DOLP indicates the crystalline alignment of fibers and molecules parallel to the linear polarization states, and that the DOCP is a measure of how effectively the medium flips the helicity of the scattered light. The DOCP parameter also determines the optical activity of collagen with SH light. Therefore, Fig. 7 highlights that the collagen fiber is highly anisotropic, with a spatial variation coinciding with the known pitches of distinct helices within the coil structures of fibers [46,47]. In this image analysis, these polarization parameters are related to the alignment of dipoles within the focal volume. Fig. 7 highlights the different morphologies of the fiber present within type-I collagen. Furthermore, Fig. 7(b) shows, that both the linearly and circularly polarized SH light is generated from different regions of type-I collagen. The DOLP and DOCP values were contrasting; the region with higher/lower DOLP value shows lower/higher DOCP value. These variations of polarization parameters are attributed to the relative phase changes between the extraordinary and the ordinary rays and the orientation of the crystals at different focal depth [17,41,47]. In the case of a collagen based structure, it is possible to produce partially polarized states of polarization due to the random distributions of molecular orientation and strong scattering. This gives rise to an averaging over all polarization states present, which can manifest itself as partial polarization. Measuring the Stokes parameters is the only way to fully characterize the polarization state. From these Stokes parameters we can reconstruct the different polarization parameters like DOP, DOLP, and DOCP. Type-I collagen, furthermore, forms cylindrical arrays of polypeptide coils comprising glycine-proline helices [48]. From the Stokes vector-S_3 and DOCP, the circular dichroism and helicity of the collagen molecules can be found, respectively.

The SH signal strength depends on the geometrical characteristics and the relative path differences between SH active molecules within the sample [1,2]. To investigate the alignment and orientation of molecules, we acquired a large variety of SH intensity patterns, by varying the polarization state of the incident laser light and detecting different polarization components of the SH signal via our PSA. As indicated in Fig. 8, the 4 ROIs (marked as black boxes in the central panel) with size of 3×3 pixels have different Stokes parameters, suggesting differing molecule orientations in these regions. Although, the Stokes parameters can measure the polarization states of SH light, they are not sufficient to unambiguously determine the alignment and orientation of molecules. To

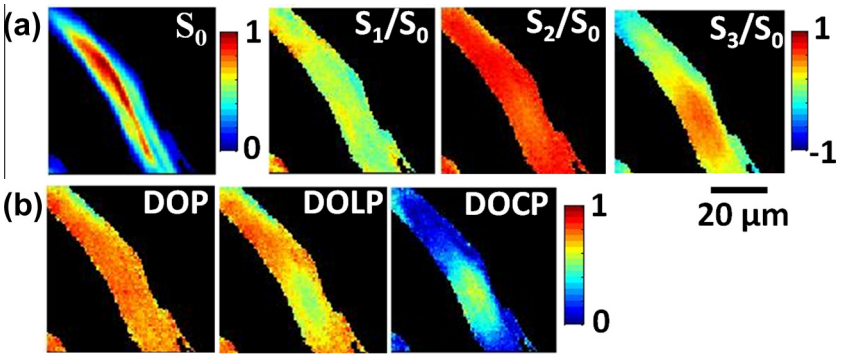

Fig. 7. Experimental polarization resolved SHG response from type-I collagen, (a) shows the reconstructed 2D Stokes vector images; (b) represents the DOP, DOLP and DOCP images of SHG light from the type-I collagen, when the input polarization is horizontal polarized. These reconstructed 2D Stokes images are taken at 50 × 50 pixel analysis without relying on any sample alignment or analyzer rotation. The color scale shows the values of each parameter.

help overcome this issue, we measured the magnitude of the each Stokes parameter whilst the (linear) polarization state of the illumination was rotated through 360° (data points were taken every 6°) as shown in Fig. 8. It has been previously been reported that SHG plots of Fig. 8 can be used to determine the orientation and the degree of organization of collagen fibers in human tissues taken from a cadaver [49,50]. In particular, the red curves in Fig. 8 show the angular dependence of total SH intensity ($S_0 = I_{0^\circ} + I_{90^\circ}$) and is seen to be very similar in all 4 ROIs. We also observe that the resultant SH intensity (S_0) is maximal at 45° for R1 and R2, and 60° for R3 and R4, when the laser polarization is parallel to the collagen fiber direction. Similarly, minima occur when the collagen fiber are n perpendicular to the incident polarization. The shape of SH intensity (S_0) is characteristic of having a uniaxial collagen orientation [49,50]. We also analyzed the angular dependence of all the Stokes parameters to characterize the molecular orientation more fully. As shown in the Fig. 8, S_1, S_2 and S_3 (blue, black and green) graphs vary between the 4 ROIs. Since, these Stokes parameters (S_1, S_2 and S_3) are the combination of $I_{0^\circ} - I_{90^\circ}, I_{45^\circ} - I_{-45^\circ}, I_{RCP} - I_{LCP}$ and variation of intensities with laser polarizations can resolve the different degree of organizations of collagen fibers. The SH intensity patterns of Stokes parameters for R1 and R2 are very similar, and R3 and R4 as well. The measured SH responses for S1 and S2 as a function of incident polarization angles show that the R1 and R2 regions are more anisotropic than R3 and R4. On the other hand, the angular dependency of Stokes vector-S_3 indicates that R3 and R4 regions are more chiral than R1 and R2. It has been reported that collagen produces strong second-order nonlinearity response results from both chiral and achiral contributions with sum-frequency generation vibrational spectroscopy [51]. The 2D reconstructed DOLP and DOCP images (in Fig. 7(b)) also highlighted the spatial distribution of anisotropic and chiral molecules in collagen as mentioned previously. We have thus observed that type-I collagen shows both chiral and achiral behavior as can be distinguished from full Stokes vector measurements. The achiral contribution to SH signal is due to the non-centrosymmetric ordering of the methylene groups of the collagen fiber [51]. In contrast, carbonyl groups associated

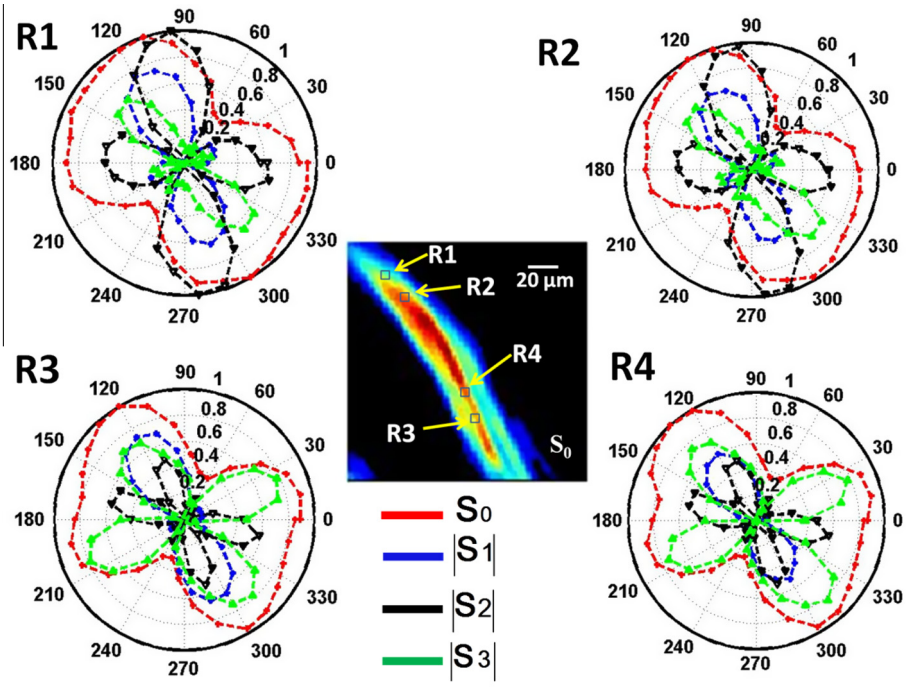

Fig. 8. Shows the graphs for absolute values of Stokes parameters as a function of incident polarization, where the data are taken every 6° in 4 ROIs as indicated in S_0 image. In each ROI, the Stokes parameters are divided by their maximum S_0 values for comparison.

with the amide I bands results in a strong chiral contribution to SH signal [52]. A difference in the Stokes parameters of SH signal is clearly observed in Fig. 7 and Fig. 8, as the angle between the laser polarization and α-helix axis is varying. This variation is, due to the α-helical protein structural arrangement within the different collagen fiber. Since S_3 is a measure of how effectively the collagen fiber flips the helicity of the scattered light from right to left handedness within the focal volume, the different values of Stoke parameters indicate the change in the polarization. Thus the chiral SHG response should depend on the variation in the contribution of chiral and achiral susceptibility elements [52]. This can, in turn reveal collagen-fiber orientation and structural order through SH detection. As shown in Fig. 7(a) and (b), the normalized Stokes vector images and the affect of polarization properties of SH signals in each pixel of thick type-I collagen are shown. Hence, Stokes vector based SH polarimetry imaging, including a variation of the incident polarization states, may provide a selective and specific contrast technique for collagen structures in tissue matrices e.g. skin lesions. Furthermore, we believe that photon counting detectors have the advantages of (1) better signal-to-noise ratio by avoiding 1/f noise, (2) better quantification of light intensity, and (3) allowing background fluorescence to be gated. The temporal resolution afforded can also be very useful in fluorescence studies.

4. Conclusion

In conclusion, this study has demonstrated the uniqueness and impact of Stokes vector based polarization resolved SHG imaging to characterize the polarization state of SH light, which is correlated with the molecular structure of KDP micro-crystals and type-I collagen. In conventional polarization microscopy the polarization states of measured signals are usually characterized with a two-channel configuration. Polarization analysis on SH microscopy is also performed in a similar manner. SH studies however have the advantage of being highly sensitive to the structural order of targeted specimens. Generally, SH polarization analysis can be carried out by Jones calculus since it can be fully polarized. However, multiple or time-lapsed scans would be required if the phase relationship between the eigen-polarization vectors is to be uncovered.

For scenarios in which light can take a more general polarization state e.g. partially polarized or unpolarized, Stokes algebra is a better choice. The Stokes polarimeter setup in this study is configured in transmission mode to suit the forward propagation of SH. A pixel by pixel image analysis based on photon counting has been implemented to reconstruct the 2D Stokes parameters of SHG images, which were then used to reconstruct DOP, DOLP, and DOCP images for visualization of the SH polarization effects in KDP micro-crystals and type-I collagen in a single measurement. The specimens were excited with a single polarization state and four intensity images detected simultaneously. The results from the Stokes polarimeter, as opposed to the two-channel setup, can be seen from Figs. 7 and 8. Notably, the SH is essentially fully polarized, due to the coherent nature of the SHG process. The linearly and circularly polarized proportions of SH, however, differ reflecting the varying structural order and domains within the collagen fibrils. This information is not easily revealed with conventional two-channel setups.

SH intensity alone, however, is not sufficient to completely reveal the structure of the SH active samples. The analysis was therefore extended to include the orientation and degree of organization from type-I collagen by varying the incident laser polarization whilst detecting the resulting polarization state of SH light using the four-channel Stokes-polarimeter. Unfortunately a full Mueller matrix formalism, a powerful method in the context of linear optics, is difficult nonlinear optics. For example, the equivalent of the Lu-Chipman decomposition and the corresponding interpretation are lacking and may be counter-intuitive. Despite this fact, we have shown that analysis of the DOP, DOLP, and DOCP provide a useful means to interpret the measured Stokes vectors and images. This technique is therefore ultimately expected to be applied in a broad variety of specimens, including biomedical tissues [53].

Acknowledgments

We appreciate greatly the help from Prof. Tsu-Wei Nee for fruitful discussions on implementing Stokes vector based methods. The authors would also like to thank the National Science Council, Taiwan (NSC99-2627-M-010-002, NSC98-2627-M-010-006, NSC97-2112-M-010-002-MY3, and NSC98-2112-M-010-001-MY3) for their generous funding.

Appendix A. Supplementary data

Supplementary data associated with this article can be found, in the online version, at http://dx.doi.org/10.1016/j.ymeth.2013.07.019.

References

[1] J. Gannaway, C.J.R. Sheppard, Opt. Quantum Electron. 10 (1978) 435–439.
[2] P.J. Campagnola, L.M. Loew, Nat. Biotechnol. 21 (2003) 1356–1360.
[3] M.L. Zheng, K. Fujita, W.Q. Chen, X.M. Duan, S. Kawata, J. Phys. Chem. C 115 (2011) 8988–8993.
[4] X. Chen, O. Nadiarynkh, S. Plotnikov, J. Campagnola Nat. Protoc. 7 (2013) 654–669.
[5] R. Tanaka, S. Fukushima, K. Sasaki, Y. Tanaka, H. Murota, T. Matsumoto, T. Araki, T. Yasui, J. Biomed. Opt. 18 (2013) 061231.
[6] D.A. Dombeck, K.A. Kasischke, H.D. Vishwasrao, M. Ingelsson, B.T. Hyman, W.W. Webb, Proc. Nat. Acad. Sci. 100 (2003) 7081–7086.
[7] R. Cicchi, S. Sestini, V. De Giorgi, D. Massi, T. Lotti, F.S. Pavone, J. Biophoton. 1 (2008) 62–73.
[8] T. Yasui, Y. Tohno, T. Araki, App. Opt. 43 (2004) 2861–2867.
[9] Y. Sun, W.L. Chen, S.J. Lin, S.H. Jee, Y.F. Chen, L.C. Lin, P.T.C. So, C.Y. Dong, Biophys. J. 91 (2006) 2620–2625.
[10] M. Han, G. Giese, J.F. Bille, Opt. Express 13 (2005) 5791–5797.
[11] P. Matteini, F. Ratto, F. Rossi, R. Cicchi, C. Stringari, D. Kapsokalyvas, F.S. Pavone, R. Pini, Opt. Express 17 (2009) 4868–4878.
[12] S.V. Plotnikov, A.C. Millard, P.J. Campagnola, W.A. Mohler, Biophys. J. 90 (2006) 693–703.
[13] M.E. Quinlan, J.N. Forkey, Y.E. Goldman, Biophys. J. 89 (2005) 1132–1142.
[14] C.P. Pfeffer, B.R. Olsen, F. Ganikhanov, F. Légaré, Opt. Express 2 (2011) 1366–1376.
[15] D. Ait-Belkacem, A. Gasecka, F. Munhoz, S. Brustlein, S. Brasselet, Opt. Express 18 (2010) 14859–14870.
[16] L. Fu, M. Gu, Opt. Express 16 (2008) 5000–5006.
[17] Rudolf Oldenbourg, Peter Török, Appl. Opt. 39 (2000) 6325–6331.
[18] R.M.A. Azzam, N.M. Bashara, Ellipsometry and Polarised Light, Elsevier, North Holland, 1987.
[19] Eugene Hecht, Optics, 4th ed., Addison Wesley, 2002.
[20] M.J. Walker, Am. J. Phys. 22 (1954) 170–174.
[21] N. Ghosh, M.F.G. Wood, I.A. Vitkin, Opt. Commun. 283 (2010) 1200–1208.
[22] N. Mazumder, J. Qiu, M.R. Foreman, C.M. Romero, C.W. Hu, H.R. Tsai, P. Török, F.J. Kao, Opt. Express 20 (2012) 14090–14099.
[23] N. Mazumder, J. Qiu, M.R. Foreman, C.M. Romero, P. Török, F.J. Kao, Opt. Express 4 (2013) 538–547.
[24] S.Y. Lu, R.A. Chipman, J. Opt. Soc. Am. A 13 (1996) 1106–1113.
[25] Y. Shi, W.M. McClain, Phys. Rev. A 49 (1994) 1999.
[26] P.A. Letnes, I.S. Nerb, L.M. Sandvik Aas, P.G. Ellingsen, M. Kildemo, Opt. Express 18 (2010) 23095–23103.
[27] J.G. Webster, "Polarization measurement", in The Measurement, Instrumentation and Sensors Handbook, CRC Press, 1998 (Chap. 60).
[28] R.M.A. Azzam, Opt. Lett. 10 (1985) 309–311.
[29] J.S. Baba, J.R. Chung, A.H. DeLaughter, B.D. Cameron, G.L. Cote, J. Biomed. Opt. 7 (2002) 341.
[30] C.W. Sun, C.C. Yang, Y.W. Kiang, Appl. Opt. 42 (2003) 750–754.
[31] M.R. Antonelli, A. Pierangelo, T. Novikova, P. Validire, A. Benali, B. Gayet, A.D. Martino, Opt. Express 18 (2010) 10200–10208.
[32] N. Ghosh, M.F.G. Wood, J. Biophotonics 2 (2009) 145–156.
[33] M.R. Foreman, C.M. Romero, P. Török, Opt. Express 16 (2008) 15212–15227.
[34] E. Compain, S. Poirier, B. Drevillon, Appl. Opt. 38 (1999) 3490–3502.
[35] S.N. Savenkov, Opt. Eng. 41 (2002) 965–972.
[36] J.S. Tyo, Appl. Opt. 41 (2002) 619–630.

[37] W. Becker, H. Hickl, C. Zander, K.H. Drexhage, M. Sauer, S. Siebert, J. Wolfrum, Rev. Sci. Inst. 70 (1999) 1835.
[38] R. Krahl, A. Bülter, F. Koberling, "Performance of the Micro Photon Devices PDM 50CT SPAD detector with PicoQuant TCSPC systems", Technical Note (PicoQuant GmbH, 2005) (2005).
[39] P. Bianchini, A. Diaspro, J. Biophoton. 1 (2008) 443–450.
[40] M.R. Foreman, P. Török, Phys. Rev. A 82 (2010) 043835.
[41] R. Gauderon, P.B. Lukins, C.J.R. Sheppard, Opt. Lett. 23 (1998) 1209–1211.
[42] P. Stoller, B.M. Kim, A.M. Rubenchik, K.M. Reiser, L.B. Da Silva, J. Biomed. Opt. 7 (2002) 205–214.
[43] G. Cox, E. Kable, A. Jones, I. Fraser, F. Manconi, M.D. Gorrell, J. Struct. Biol. 141 (2003) 53–62.
[44] T. Verbiest, S.V. Elshocht, M. Kauranen, L. Hellemans, J. Snauwaert, C. Nuckolls, T.J. Katz, A. Persoons, Science 282 (1998) 913–915.
[45] M. Shribak, R. Oldenbourg, Appl. Opt. 42 (2003) 3009–3017.
[46] J.C. Mansfield, C.P. Winlove, J. Moger, S.J. Matcher, J. Biomed. Opt. 13 (4) (2008) 044020.
[47] S. Psilodimitrakopoulos, I. Amat-Roldan, P. Loza-Alvarez, D. Artigas, Opt. Express 3 (2012) 2681–2693.
[48] M. Wolman, F.H. Kasten, Histochemistry 85 (1986) 41–49.
[49] T. Yasui, Y. Tohno, T. Araki, Appl. Opt. 43 (2004) 2861–2867.
[50] T. Yasui, Y. Tohno, T. Araki, J. Biomed. Opt. 9 (2004) 259–264.
[51] I. Rocha-Mendoza, D.R. Yankelevich, M. Wang, K.M. Reiser, C.W. Frank, A. Knoesen, Biophys. J. 93 (2007) 4433–4444.
[52] K.M. Reiser, A.B. McCourt, D.R. Yankelevich, A. Knoesen, Biophys. J. 103 (10) (2012) 21772–21786.
[53] A.M. Pena, T. Boulesteix, T. Dartigalongue, M.C.S. Klein, J. Am. Chem. Soc. 127 (2005) 10314–10322.